SCA-9834

The "Spinning Disk" Approach to Capillary Pressure Measurement with a Centrifuge Experiment

Salah M. Al-Modhi, and Richard L. Christiansen
Petroleum Engineering Department
Colorado School of Mines

ABSTRACT

The "spinning disk" approach to measurement of capillary pressure was first proposed almost 10 years ago, but the method has never been tested. In this paper, the theoretical foundation of the method will be described, and the first experimental observations will be presented.

In the spinning disk approach, a cylindrical sample of porous material is spun on its axis of symmetry. That is, the axis of the rotor is the same as the axis of symmetry of the cylindrical specimen. This approach is markedly different from the standard centrifuge experiment in which the material is spun at some distance (usually about 10 cm) from the axis of the rotor. An advantage of the spinning disk method is that large samples of porous material can be easily tested. In fact, large diameter samples are preferred.

In this paper, the capillary pressure relationship is obtained in two ways from the experimental observations. First, the relationship is calculated from a set of average saturations measured at different spin rates. The expression for processing the data is the truncated Hassler-Brunner expression. For the spinning disk geometry, the truncated expression is precisely correct. Secondly, the capillary pressure relationship is obtained with direct visual methods that were first demonstrated in our laboratory in 1997.

CONCEPTUAL BACKGROUND

Centrifuge experiments have been used for measuring capillary pressure relationships since the publication of Hassler and Brunner(1945). In the Hassler-Brunner apparatus, drawn in Figure 1, a cylindrical rock sample is spun at some distance r_i from the axis of the centrifuge. Hassler and Brunner derived an approximate expression for converting the experimentally observed data into the desired capillary pressure relationship:

$$S_w(P_{ci}) \cong S_{w,avg} + P_{ci}\frac{dS_{w,avg}}{dP_{ci}} \qquad (1)$$

Two important assumptions were needed to obtain Eq. 1. First, the rock sample must be homogeneous. Second, the centrifugal acceleration is parallel to the cylindrical axis of the sample.

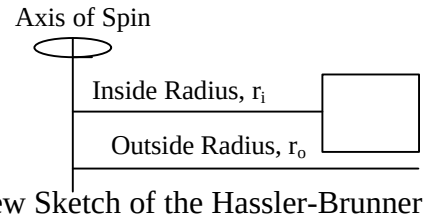

Figure 1. Side-View Sketch of the Hassler-Brunner Centrifuge Apparatus.

Erroneous capillary pressure relationships caused by failure of the first assumption are rarely discussed in the literature. Error caused by failure of the second assumption is discussed in the literature of the last ten years. But, most of the literature has focused on deriving a data processing algorithm that is more accurate than Eq. 1. A good summary of the discussion may be found in Ayappa *et al*.(1989) and Chen(1996).

While investigating the error caused by failure of the second assumption, Christiansen and Cerise(1987) found that an alternative rotor geometry, which they termed the "spinning disk" geometry, provided an interesting perspective on the Hassler-Brunner expression. To gain this perspective, consider drainage of liquid and invasion of gas for the spinning disk geometry of Figure 2.

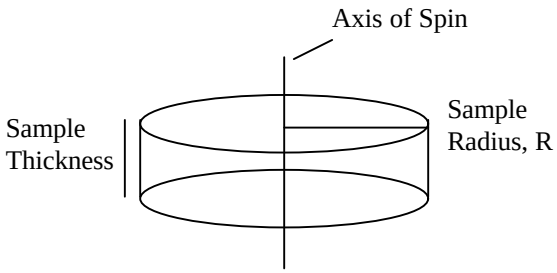

Figure 2. Sketch of the “Spinning Disk” Experiment.

If the rock sample is homogeneous, then the average liquid saturation is

$$S_{w,avg} = \frac{1}{pR^2}\int_0^R S_w(r,w)2prdr \qquad (2)$$

The variable of integration can be changed from r to P_C, noting that

$$dP_c = -\Delta r w^2 r dr ,$$

$$P_c(r=0)=\frac{1}{2}\Delta\rho w^2 R^2 =: P_{c0}\text{, and}$$
$$P_c(r=R)=0\,.$$

The second boundary condition above states that capillary pressure is zero on the cylindrical surface of the disk – the standard outlet boundary condition for centrifuge experiments. Then, after some rearrangement, Eq. 2 becomes

$$S_{w,avg}P_{c0}=\int_0^{P_{c0}} S_w(P_c)\,dP_c \qquad (3)$$

Differentiating Eq. 3 with respect to P_{c0} yields the following expression for the liquid saturation:

$$\frac{d}{dP_{c0}}\left(S_{w,avg}P_{c0}\right)=S_w(P_{c0}) \qquad (4)$$

While Eq. 1 for the standard geometry is approximate, Eq. 4 is exact for the spinning disk geometry. The source of the error in Eq. 1 is revealed by repeating the above analysis, in brief, for the standard geometry. For the standard geometry, the average saturation is

$$S_{w,avg}=\frac{1}{L}\int_0^L S_w(r,w)\,dr \qquad (5)$$

Using the following expressions to change variables from r to P_c,

$$dP_c=-\Delta\rho w^2 r\,dr\ ,$$
$$P_c(r=r_i)=\frac{1}{2}\Delta\rho w^2 R\left(r_o^2-r_i^2\right)=:P_{ci}\ \text{, and}$$
$$P_c(r=r_o)=0\ ,$$

then, the following expression is obtained:

$$S_{w,avg}P_{ci}=\frac{r_i+r_o}{2}\int_0^{P_{Ci}}\frac{S_w(P_c)}{r}\,dP_c \qquad (6)$$

Differentiation of Eq. 6 with respect to P_{ci} yields an expression complicated by the presence of r in the denominator of the integrand of Eq. 6:

$$\frac{d}{dP_{Ci}}\left(S_{w,avg}P_{ci}\right)=\frac{(r_i+r_o)}{2r_i}S_w(P_{ci})+\frac{(r_i+r_o)}{2}\int_0^{P_{Ci}}\frac{d}{dP_{ci}}\left[\frac{S_w(P_c)}{r}\right]dP_c \qquad (7)$$

It appears that the root of error in Eq. 7 is non-conformance of the standard geometry to the radial nature of the centrifugal field. The spinning disk conforms to the radial centrifugal field; the standard geometry does not. Hassler and Brunner(1945) suggested that the ratio r_i/r_o should be greater than 0.7 to minimize the error of truncating Eq. 7 to Eq. 1. According to the Hassler-Brunner recommendation for r_i/r_o, a short cylindrical sample (a disk) is preferred for the standard geometry. Such could not be further from the truth. Indeed, Christiansen(1992) showed that a better expression for guiding the selection of rock diameter and length is the following dimensionless geometric indicator:

$$N_{gi} = \left(\frac{R}{L}\right)^2 \left(\frac{r_o - r_i}{r_o + r_i}\right) \tag{8}$$

Here, *R* is the radius of the sample, and *L* is its length. Christiansen and Cerise(1987), Christiansen(1992), and Forbes *et al*.(1994) have shown that N_{gi} is an approximate indicator of fractional error in data processing. For example, if N_{gi} equals 0.05, then the capillary pressure relationship obtained by processing the centrifuge data differs from the correct relationship by about 5%. According to Eq. 8, a long, small diameter rock sample is preferred.

The above analysis shows that data processing for the spinning disk geometry is simpler and more precise than for the standard geometry. Nevertheless, there is no documented use of this new geometry in the literature. Apparatus and experimental results for a first implementation of the geometry are described below.

APPARATUS AND PROCEDURES

A sketch of the sample cell with collection vessels for the spinning disk experiments appears in Figure 3. The sample cell was constructed of pieces of polyacrylic sheet, bonded together with ethylene dichloride. Those parts of the sample cell that must be removed occasionally are held to the rest of the cell with machine screws. Silicone rubber cement is used to seal those joints as needed. As described in a companion paper in these proceedings (Al-Omair and Christiansen, 1998), construction of centrifuge cells from plastic allows for great flexibility in testing new designs. The sample cell was bolted to the rotor assembly as shown in Figure 4. The large diameter plate (polycarbonate) provides additional rotary stability. The rotor shaft is machined to mate with the axle of a Beckman J6-B centrifuge.

The sample cell used in experiments to date does not allow for consolidated samples. Just sandpacks and glass-bead packs have been tested. The unconsolidated material is maintained in the circular sample chamber with 150 mesh screens as shown in Fig. 3. The next version of the sample holder will accommodate consolidated samples.

.

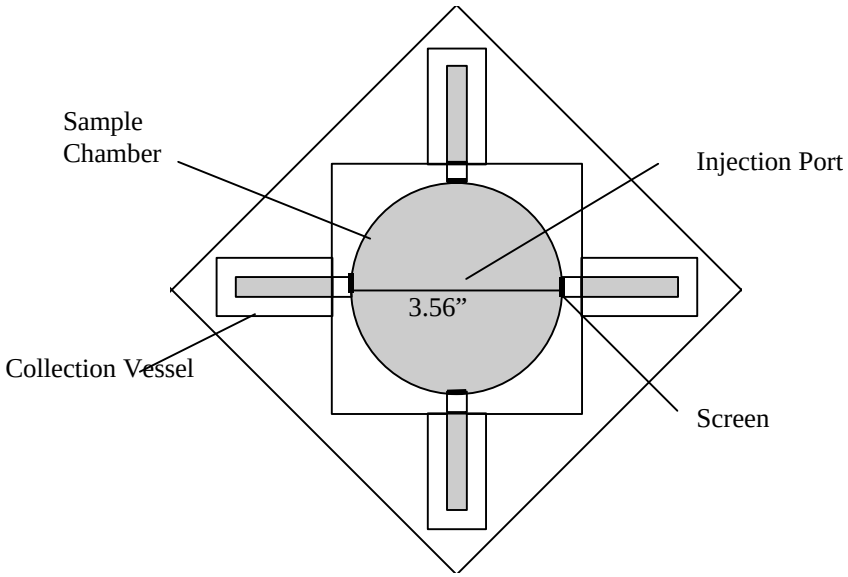

Figure 3. Sample Cell for Spinning Disk Experiment.

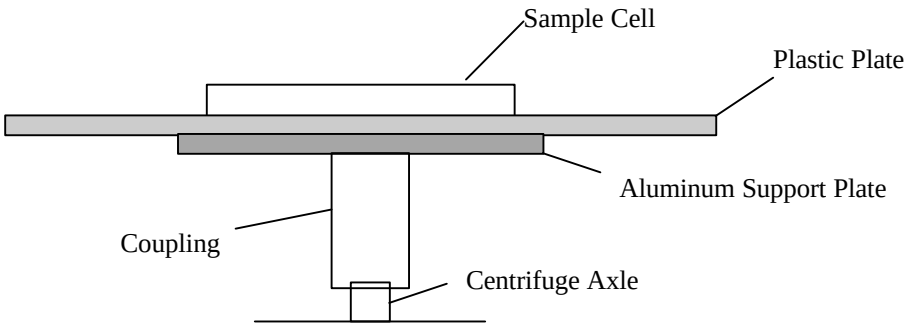

Figure 4. Sample Cell Mounted on Rotor in Centrifuge.

One complication that has arisen in experiments with the sample cell of Figure 3 is that drainage to the four collection vessels is not equal. That is, one of the collection vessels accumulates more liquid than the others. This unequal collection requires temporary termination of an experiment in order to remove excess liquid. We believe that unequal accumulation results from unequal resistance to flow through the screens that prevent radial settling of the sand pack. We anticipate that with consolidated samples, with the screens removed, that unequal accumulation may not be as severe. We have considered connecting the collection vessels with a common line to equalize liquid levels.

At the start of an experiment, the sandpack or glass-bead pack is saturated with dyed water by injecting the liquid through a small hole in the center of the sample chamber. The initial liquid saturation is calculated from the difference in mass of the dry and saturated condition. Typically, the initial liquid saturation is about 95%. For these preliminary tests of the spinning disk apparatus, initial liquid saturations less than 100% were considered acceptable.

Video images, before and after the sandpack or glass-bead pack is saturated, are recorded with a video camera connected through a VCR to a computer. Image analysis software is used to develop a correlation between the gray level of the image and saturation. For example, the gray level of the dry sandpack image corresponds to zero liquid saturation S_w. Details of the video imaging method may be found in the thesis of Al-Omair(1997). A sample video image is shown in Figure 5.

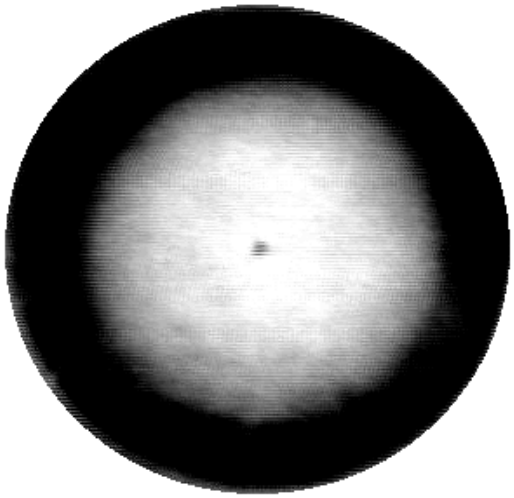

Figure 5. A video image of the sandpack.

RESULTS AND DESCUSION

Properties of the sandpack and glass-bead packs are shown in Table 1. Permeabilities and threshold pressures were measured for the three media in a separate apparatus; nevertheless, the values should be approximately the same for the media packs in the spinning disk apparatus.

Table 1. Properties of Porous Media.

Porous Medium	Porosity, %	Permeability, Darcies	Threshold Pressure, psi
20-40 Mesh Sand Pack	32	154	0.25
80-120 Mesh Glass-bead Pack	39	24	0.55
120-170 Mesh Glass-bead Pack	39	8.5	0.85

Capillary pressure relationships measured with the spinning disk apparatus for sandpacks and glass-bead packs are shown in Figures 6, 7, and 8. Both the "raw" average saturation and the local saturation relationships are shown. The local saturations were obtained by applying Eq. 1 to the average saturation data. Threshold pressure for the three packs is detectable from the centrifuge experiment, as demonstrated in these figures. These threshold pressures agree with those in Table 1 that were measured in a separate apparatus. The capillary pressure relationship obtained for the 20-40 Mesh Sandpack is approximately the same as those reported by Al-Omair(1997), and Al-Omair and Christiansen(1998) for the same media.

The capillary pressure relationship obtained from the video measurements for the 20-40 Mesh Sand Pack is shown in Figure 9. For liquid saturations greater than 0.2, the video results agree with the results obtained by differentiating the average saturation data with Equation 1. Further refinement of the experimental technique is necessary to resolve the differences at low liquid saturations.

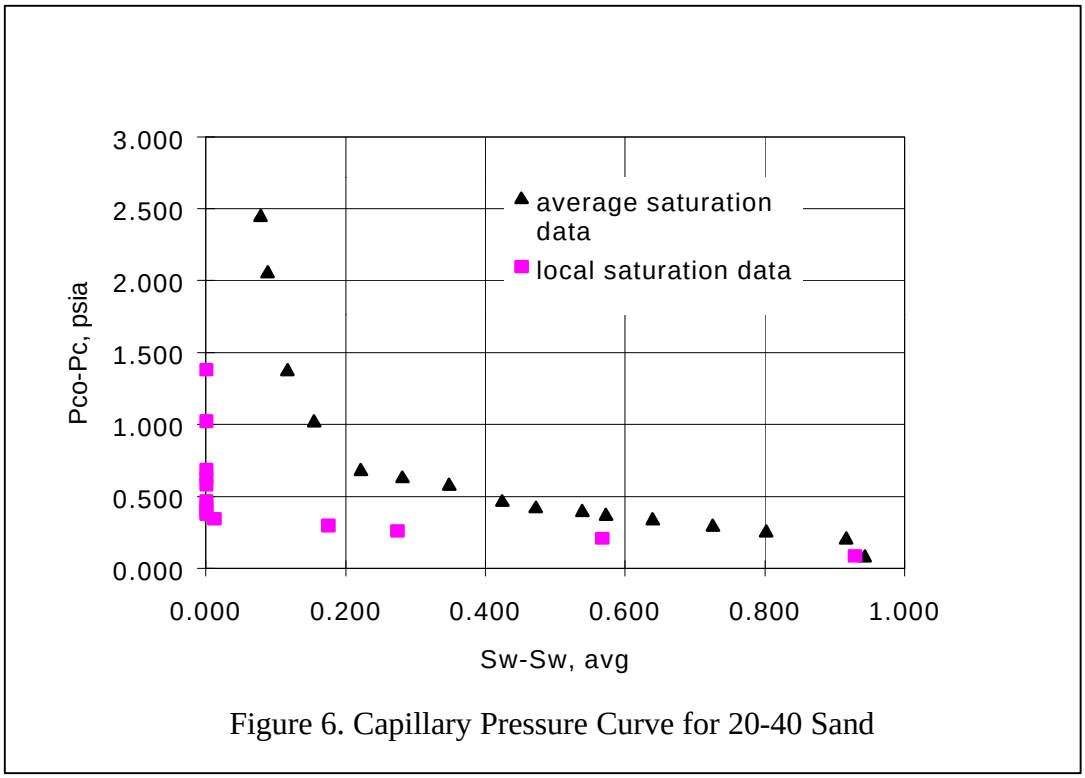

Figure 6. Capillary Pressure Curve for 20-40 Sand

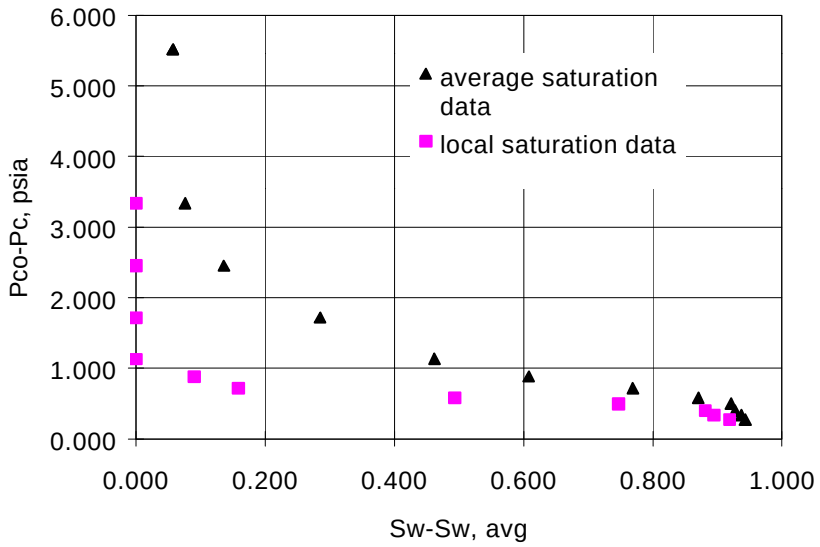

Figure 7. Capillary Pressure Curve for 80-120 Glass-Beads

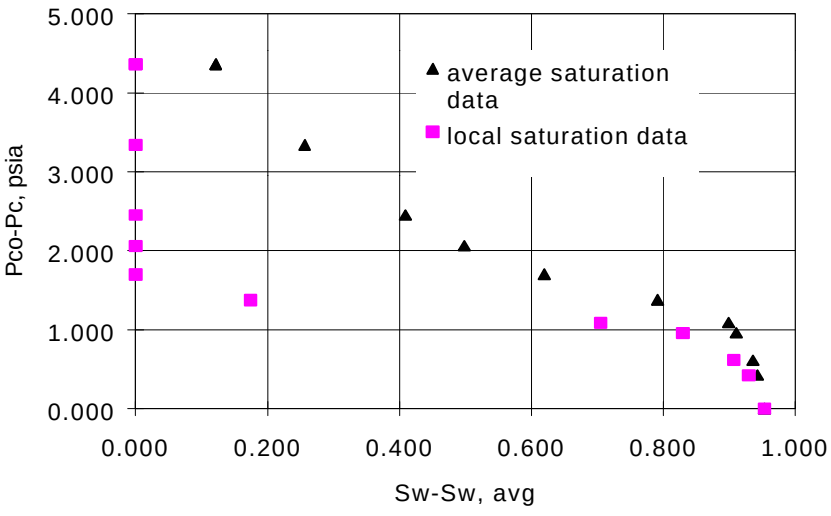

Figure 8. Capillary Pressure Curve for 100-170 Glass-Beads

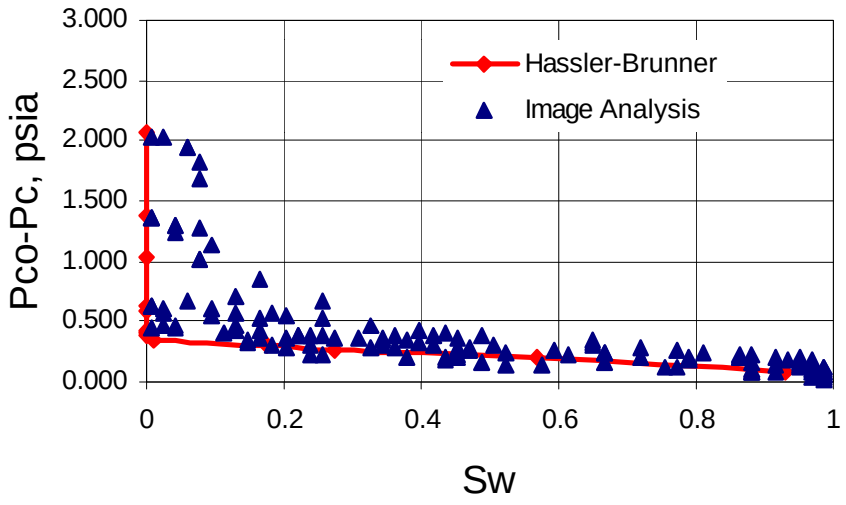

Figure 9. Measured Capillary Pressure Relationship for 20-40 Sand pack

CONCLUSIONS

1. The geometry of the spinning disk approach to measurement of capillary pressure yields an exact expression for obtaining local saturation by differentiation of the average saturation data.
2. Large diameter samples can be used in the spinning disk method. In fact, they are preferred.
3. Threshold pressures measured with the spinning disk method agree with those measured with other methods.
4. The capillary pressure relationship obtained with the spinning disk method is the same as that obtained with the standard geometry.
5. Currently, the video method of obtaining capillary pressures for the spinning disk apparatus is successful for liquid saturations greater than about 0.2.

NOMENCLATURE

L = length of sample
P_c = capillary pressure
P_{ci} = capillary pressure at the inner face of the sample in the standard geometry
P_{c0} = capillary pressure at the center of the sample in the spinning-disk geometry
r = radius

r_i = radial distance to the inner face of the sample in the standard geometry
r_o = radial distance to the outer face of the sample in the standard geometry
R = radius of sample
S_w = local water saturation
$S_{w,avg}$ = average water saturation for entire sample
$\Delta\rho$ = fluid mass density difference
ω = centrifuge angular velocity

REFERENCES

Al-Omair, O. A., "Video Imaging Method for Determining the Capillary Pressure Relationship with a Centrifuge," MS Thesis, Colorado School of Mines, Golden, CO, 1997.

Al-Omair, O. A., Christiansen, R. L., "Measurement of Capillary Pressure by Direct Visualization of a Centrifuge Experiment," Presented at 1998 SCA Technical Conference, The Hague, September 14-16.

Ayappa, K.G., Davis, H.T., Davis, E.A., and Gordon, J., "Capillary Pressure: Centrifuge Method Revisited," *AIChE J*., (1989) **35**, 365-375

Chen, Z. A., "Centrifuge Capillary Pressure Curve Measurements: Theory and Physics," Ph. D. Dissertation, University of Manitoba, Winnipeg, Manitoba, 1996.

Christiansen, R. L., "Geometric Concerns for Accurate Measurement of Capillary Pressure Relationships with Centrifuge Methods," *SPE Form. Eval*., (December 1992),311-314.

Christiansen, R. L., and Cerise, K. S., "Capillary Pressure: Reduction of Centrifuge Data," Paper 47d presented at the 1987 AIChE Annual Meeting, New York City, November 15-20.

Forbes, P.L., Chen, Z.A., and Ruth, D.W., "Qualitative Analysis of Radial Effects on Centrifuge Capillary Pressure Curves," SPE 28182, provided to the Society of Petroleum Engineering, (January 1994).

Hassler, G. L., and Brunner, E., "Measurement of Capillary Pressures in Small Core Samples," *Trans*., AIME (1945) **160**, 114-123.